Improved estimates of forest cover and loss in the Brazilian Amazon in 2000–2017

Yuanwei Qin[1], Xiangming Xiao[1*], Jinwei Dong[2*], Yao Zhang[1], Xiaocui Wu[1], Yosio Shimabukuro[3], Egidio Arai[3], Chandrashekhar Biradar[4], Jie Wang[1], Zhenhua Zou[1], Fang Liu[2], Zheng Shi[1,6], Russell Doughty[1] and Berrien Moore III[5]

[1] Department of Microbiology and Plant Biology, Center for Spatial Analysis, University of Oklahoma, Norman, OK, USA. [2] Institute of Geographic Science and Natural Resource Research, Chinese Academy of Sciences, Beijing, China. [3] Brazilian National Institute for Space Research, São José dos Campos, Brazil. [4]International Center for Agricultural Research in the Dry Areas, Cairo, Egypt. [5] College of Atmospheric and Geographic Sciences, University of Oklahoma, Norman, OK, USA. [6]Present address: Co-Innovation Center for Sustainable Forestry in Southern China, College of Biology and the Environment, Nanjing Forestry University, Nanjing, China. *e-mail: xiangming.xiao@ou.edu; dongjw@igsnrr.ac.cn

Abstract

The data, information and knowledge on the tropical forest area and its dynamics in the Brazilian Amazon remain contentious. We use time-series satellite images to quantify annual forest area, loss and gain in the Brazilian Amazon during 2000–2017. We find that forest area was ~15% higher than the estimate by the official Brazilian forest dataset (PRODES), but annual forest-loss rates were twice the PRODES estimates (~0.027×10^6 km^2 yr^{-1} during 2001–2016). Forest-loss rates increased again after 2013. The El Niño and drought year (2015/2016) drove large forest area loss. The cumulative forest-loss area within the protected areas (which include ~50% of forests in the region) was ~11% of the total forest-loss area, which highlights the roles of protected areas in forest conservation.

Introduction

The area, spatial distribution and annual dynamics of tropical forests substantially affect biodiversity, terrestrial carbon cycle, hydrology and climate at local, regional and global scales[1,2]. As the world's largest tropical forest and most biodiverse terrestrial ecosystem[3], the Amazon Basin is a priority area for global conservation and warrants precise monitoring of anthropogenic impacts. Rapidly changing climate, land use, disturbances (for example, fire) and human activity in the Amazon Basin have resulted in substantial deforestation over the past several decades[4,5].

Several studies have generated maps of forest in the Amazon through analyses of space-borne optical images at various spatial resolutions, including coarse (≥1 km; for example, the Advanced Very High Resolution Radiometer (AVHRR)[6] and Satellite Pour l'Observation de Ia Terre 4 (SPOT-4) VEGETATION[7]), moderate (≥100 m; for example, Moderate Resolution

Imaging Spectroradiometer (MODIS)[8,9]) and fine (≥10 m; for example, Landsat[10,11]) resolutions. However, these Amazon forest maps have large uncertainties and have sparked intense debate due to image data availability, image data quality (cloud cover, shadows and fire-induced atmospheric contamination), mapping algorithms, forest definition, minimum mapping unit, etc.[12,13,14]. Forest area, spatial distribution, temporal dynamics and annual rates of forest loss have been contentious for decades[12,15,16]. Two recent studies[15,17] reported that both the official Brazilian deforestation dataset (PRODES)[18] and Global Forest Watch (GFW)[11] missed relatively large areas of forest loss. For instance, approximately 9,000 km^2 of forest loss was not reported by the PRODES dataset for 2008–2012 due to the 6.25-ha minimum mapping unit[15]. These staggering omissions show the need for more accurate annual Amazon forest maps and improved analyses of forest area, spatial distribution and annual dynamics to support the scientific, legislative and land management communities who strive to better understand and conserve rainforests in Brazil.

Space-borne Synthetic Aperture Radar (SAR) technology has made notable progress in the past decade and has also been useful in forest mapping[13]. SAR images, especially the L-band SAR images, can penetrate clouds and smoke haze to interact with tree trunks and branches and differentiate forests from non-forest biomes[13]. A number of recent studies demonstrated the potential of SAR images from the Advanced Land Observing Satellite (ALOS) Phased Array Synthetic Aperture Radar (PALSAR) to identify and map forests[19,20]. However, those forest maps produced by using only PALSAR images often contained commission errors due to buildings, houses and rocks[21].

Several studies have reported the potential of combining PALSAR and optical images (MODIS, Landsat) to map tropical forests[12,13]. Time-series optical images (for example, MODIS and Landsat) can capture the seasonal and interannual variation of vegetation canopy. Satellites acquiring daily images have a much higher probability of cloud-free observations[22]. Compared to Landsat with its 16-d repeat cycle at 30-m spatial resolution, MODIS sensors onboard the Terra and Aqua satellites have a daily repeat cycle at 250-m, 500-m and 1-km spatial resolution that offers more cloud-free observations in a year. MODIS data have therefore been used to track the temporal dynamics of various land cover types and transitions in the Brazilian Amazon since 2000 (refs. [23,24,25]). We developed the Forest-MODIS and Forest-PALSAR/MODIS mapping tools, which use time-series image data and algorithms to identify forests and applied them to generate forest and evergreen forest maps for the pantropical zone[26,27], China[28], monsoon Asia[27] and South America[12].

In this study, our first objective was to more accurately map annual forest area in the Brazilian Amazon (Supplementary Fig. 1). We combined PALSAR images at 50-m spatial resolution (Fig. 1a) and MOD13Q1 (Vegetation Indices 16-Day L3 Global 250 m) images during 2007–2010, and we used the Forest-

PALSAR/MODIS mapping tool[12] to generate annual maps of tropical forests (both evergreen and deciduous) in the Brazilian Amazon (Fig. 1a,b). The resultant annual PALSAR/MODIS maps of forests at 50-m spatial resolution during 2007–2010 were compared with the official forest statistics from PRODES and other available forest map products (see Methods). Our second objective was to better understand the annual dynamics of forest area loss and gain (deforestation, reforestation and afforestation) in the region during 2000–2017. We generated annual evergreen forest maps for 2000−2017 (named as MOD100; Fig. 1c) by applying a simple and robust Forest-MODIS algorithm (see Methods) to time-series MOD09A1 (Surface Reflectance 8-Day L3 Global 500 m) data for each year[26,27]. We analysed the resultant annual evergreen forest maps to quantify the annual dynamics of forest area loss and gain within the Brazilian Amazon, states and protected areas. Finally, we investigated the trajectories of forest area loss and gain as well as their driving factors.

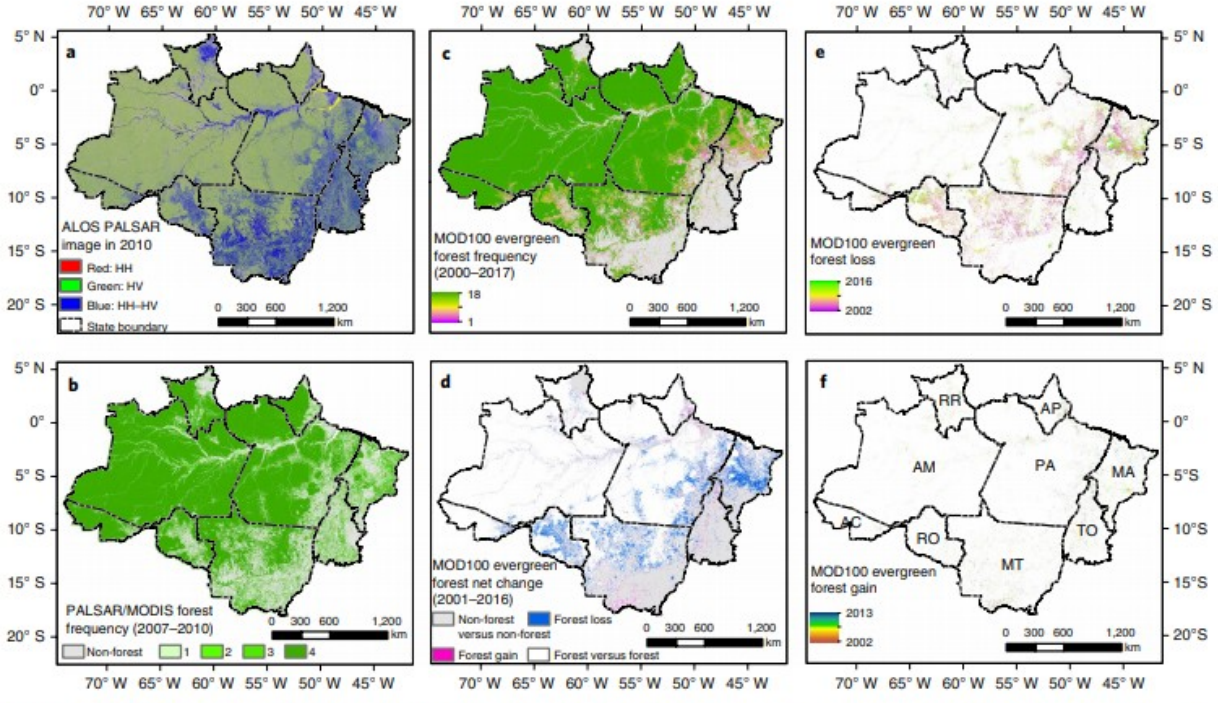

Fig. 1 | Spatial distributions of forests in the Brazilian Amazon during 2000−2017. a, A false-colour composite map of PALSAR HH (Red), HV (Green) and HH–HV (Blue) images in 2010. **b**, A frequency map of tropical PALSAR/MODIS forests in 2007−2010 (frequency values from 0 to 4) derived from the Forest-PALSAR/MODIS algorithm. **c**, A frequency map of MOD100 evergreen forests in 2000−2017 (frequency values from 0 to 18) derived from the Forest-MODIS algorithm. **d**, The net change of MOD100 evergreen forests between 2001 and 2016. **e**, The first year MOD100 evergreen forest loss (deforestation) occurred. **f**, The first year MOD100 evergreen forest gain (reforestation and afforestation) occurred. AM, Amazonas; PA, Pará; MT, Mato Grosso; AP, Amapá; RR, Roraima; AC, Acre; RO, Rondônia; TO, Tocantins; MA, Maranhão. PALSAR and MOD13Q1 (ref. [59]) images were combined to generate the PALSAR/MODIS forest (**b**). Time-series MOD09A1 land surface reflectance images[60] were used to generate MOD100 forest maps (**c**–**f**). Credit: Japan Aerospace Exploration Agency (JAXA) retains ownership of the PALSAR dataset used in **a** and **b**; USGS/NASA Landsat Programme (**b**–**f**).

Results

Annual estimates of forest area in 2007–2010

Forest area estimates from the PALSAR/MODIS forest dataset ranged from ~3.77×10^6 km^2 in 2007 to ~3.75×10^6 km^2 in 2010 (Fig. 1a,b). We compared the Brazilian Amazon forest maps for 2010 from seven data products (Supplementary Fig. 2) to illustrate the differences between the forest data products and to explore the potential of improving estimates of annual forest area in the Brazilian Amazon by integrating optical and SAR imagery and new algorithms (Fig. 2a and Supplementary Table 1). The PRODES dataset estimated 3.28×10^6 km^2 forest in 2010. Depending on the percentage of tree cover threshold values used, the forest area estimates from the GFW dataset[11] ranged from 3.71×10^6 km^2 (≥60% threshold), 3.88×10^6 km^2 (≥45% threshold), 3.97×10^6 km^2 (≥30% threshold) to 4.05×10^6 km^2 (≥10% threshold) in 2010. Our previous study[12] suggested that a 30–60% tree cover threshold was appropriate for estimating forest area from the GFW dataset when compared to forest maps derived from the PALSAR microwave images, which used a definition of forest (10% tree cover) by the UN Food and Agriculture Organization (FAO). The JAXA dataset reported 3.69×10^6 km^2 of forest in 2010. The forest area in 2010 from our PALSAR/MODIS forest map was 3.75×10^6 km^2 in the Brazilian Amazon, approximately ~2% higher than the JAXA dataset, which only used the PALSAR images[19], ~10% higher than the MODIS land cover dataset (MCD12Q1)[9], ~12% higher than the European Space Agency (ESA) Climate Change Initiative (CCI) land cover dataset[29] and ~15% (470,000 km^2) higher than the PRODES dataset[18]. These various forest area estimates highlight the discrepancies between the data products (Fig. 2a).

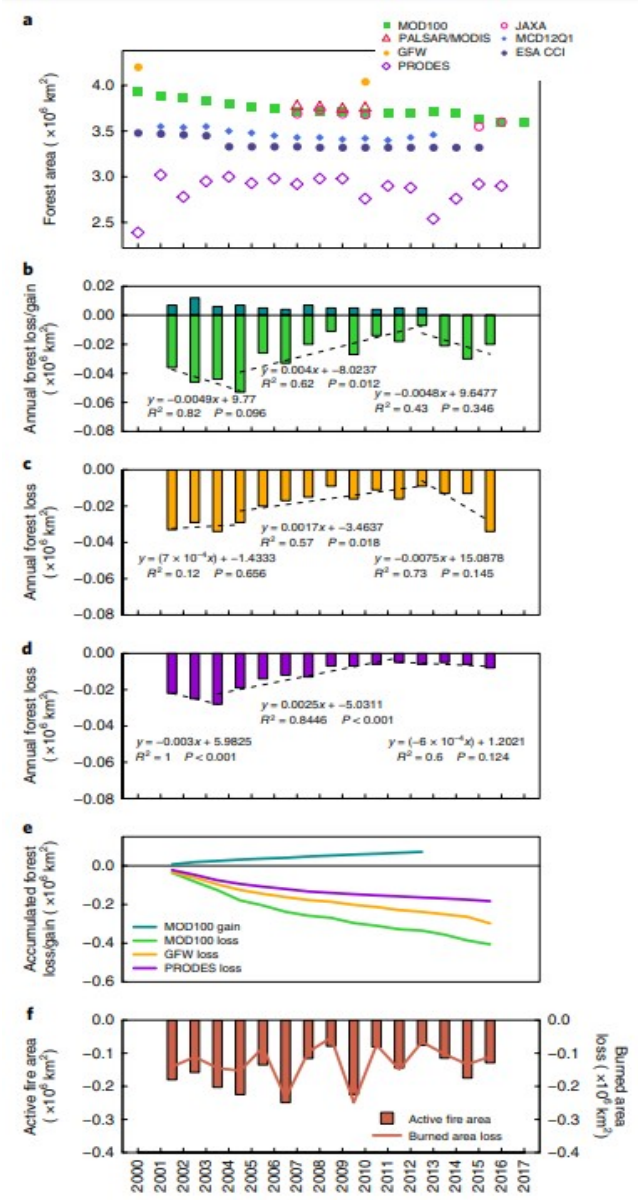

Fig. 2 | Annual dynamics of forest areas in the Brazilian Amazon during 2000–2017. a, Annual dynamics of tropical forest areas in the Brazilian Amazon during 2000–2017, as estimated from seven forest data products: (1) MOD100 (2000–2017), (2) Forest-PALSAR/MODIS (2007–2010), (3) GFW, 2000, 2010, tree cover ≥45%), (4) PRODES (2000–2016), (5) Forest-JAXA (2007–2010), (6) MCD12Q1 (2001–2013) and (7) ESA CCI (2000–2015). **b–d**, Annual evergreen forest gain and loss during 2001–2016 from the MOD100 dataset (**b**), from the GFW dataset (**c**) and from the PRODES dataset (**d**). **e**, Accumulated forest loss and gain during 2001–2016. **f**, Annual active fire and burned area from MOD14A2 and MCD64A1 during 2001–2016. Interannual variation of annual forest loss was divided into three periods, and for each period we performed a simple linear regression model (dotted lines) and reported its R^2 and P values (**b–d**).

Annual estimates of evergreen forest areas in 2000–2017

We used the MOD100 dataset to investigate the spatial distribution and annual dynamics of evergreen forests in the Brazilian Amazon. Annual evergreen forest area from the MOD100 dataset ranges from 3.72×10^6 km^2 in 2007 to 3.70×10^6 km^2 in 2010, only 1−2% lower than the forest area estimates from the Forest-PALSAR/MODIS dataset (Fig. 2a). A spatial-temporal comparison between the MOD100 dataset and the Forest-PALSAR/MODIS dataset in 2007–2010 demonstrates the robustness of the Forest-MODIS algorithm and the reliability of the MOD100 dataset in the Brazilian Amazon (Supplementary Fig. 3 and Supplementary Table 2). We also compared the MOD100 dataset with the MCD12Q1, which uses MODIS images and defines forest as tree cover >60% with a tree height >2 m. The MCD12Q1 reports 3.42×10^6 km^2 forests in 2010. The improvement of the MOD100 dataset over the MCD12Q1 dataset makes it possible to further investigate annual evergreen forest losses and gains in the Brazilian Amazon during 2000–2017.

Annual loss of evergreen forest area

Annual evergreen forest area declined from 3.93×10^6 km^2 in 2000 to 3.59×10^6 km^2 in 2017 (Figs. 1d and 2a), a net loss of 0.34×10^6 km^2 (~20,000 km^2 yr^{-1}) or about 9% of the total evergreen forest area in 2000. To reduce commission and omission errors, we excluded the first (2000) and last (2017) year and analysed MOD100 annual evergreen forest loss during 2001–2016. The result showed a cumulative loss of 0.41×10^6 km^2 (Fig. 1e), which was much larger than the estimates from the GFW (0.30×10^6 km^2) and PRODES (0.18×10^6 km^2) datasets. On average, the MOD100-estimated rate of annual evergreen forest loss was 0.027×10^6 km^2 yr^{-1}, close to five times the size of the Federal District (5,780 km^2) in Brazil.

The trajectory of annual forest area loss over time has been widely used for determining land cover and land-use change, conservation policies, management practices and identifying the socio-economic drivers of annual forest area dynamics[2,4,5]. The MOD100, GFW and PRODES datasets show three distinct phases of deforestation within the last two decades (Fig. 2b–d): (1) an initial phase of increasing forest loss (2001−2004), (2) a phase of decreasing forest loss (2005−2013) and (3) a current phase of increasing forest loss (2013−2016). All three datasets show a substantial and significant ($P < 0.05$) decreasing trend (Fig. 2b–d) of forest area loss in the second phase due to enforcement of public policy and interventions in the beef and soya markets[5]. During 2013-2016, both the GFW and MOD100 datasets showed a substantial increase in the deforestation rate, 7.5×10^3 km^2 yr^{-1} and 4.8×10^3 km^2 yr^{-1}, respectively. However, the PRODES dataset shows a much smaller increase of 0.6×10^3 km^2 yr^{-1}.

Hot-spots of evergreen forest area loss

We analysed the MOD100 dataset and identified evergreen forest loss during 2001−2016 for individual pixels geographically (Fig. 1e). The hot-spots were distributed in the ‘Arc of Deforestation’, which spans the Brazilian states of

Para (PA, 0.11 × 10^6 km^2), Mato Grosso (MT, 0.11 × 10^6 km^2), Maranhao (MA, 0.087 × 10^6 km^2) and Rondonia (RO, 0.052 × 10^6 km^2) (Fig. 3). The total forest loss in these four states accounted for approximately 87% of the total evergreen forest area loss in the Brazilian Amazon. Using a 5-km buffer in a geospatial analysis, we found that over 90% of deforestation occurred in close proximity to those areas deforested before 2002, which indicated the degree of anthropogenic activities driving the spatial dynamics of deforestation expansion (forest loss) in the Brazilian Amazon (Fig. 4).

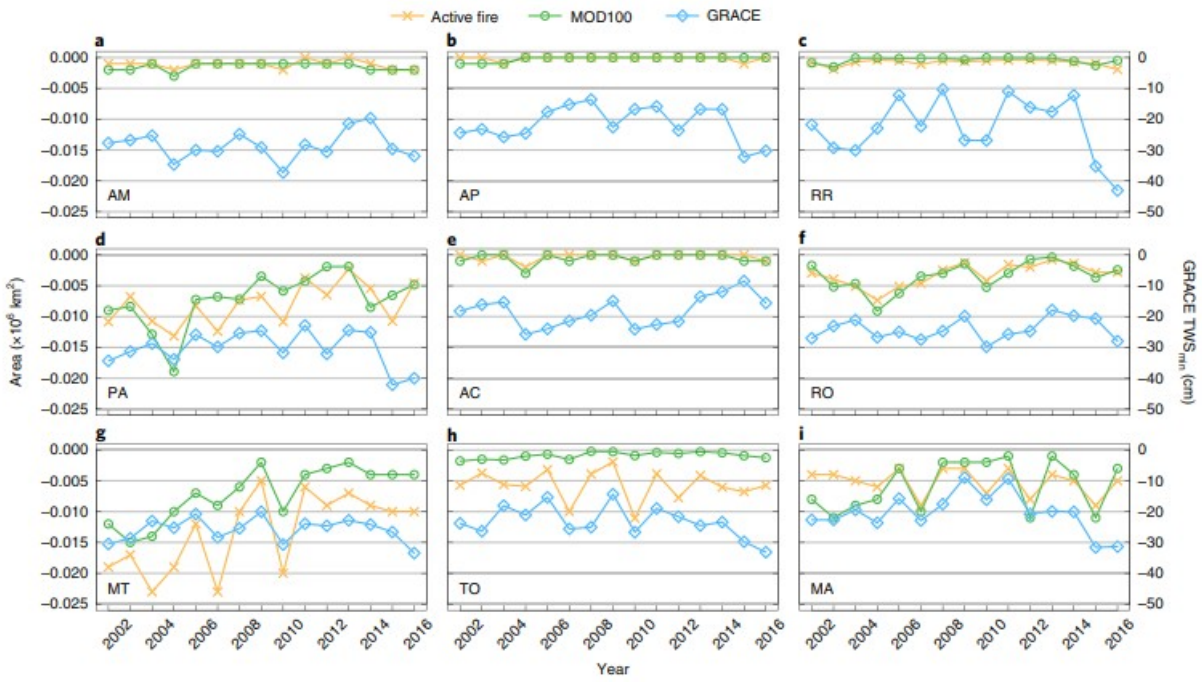

Fig. 3 | State-level forest loss, fire and water storage in the Brazilian Amazon during 2002–2016. Annual area of the MOD100 evergreen forest loss and active fire from MOD14A2, and the annual minimum terrestrial water storage (TWS_{min}) from GRACE for AM (**a**), AP (**b**), RR (**c**), PA (**d**), AC (**e**), RO (**f**), MT (**g**), TO (**h**) and MA (**i**).

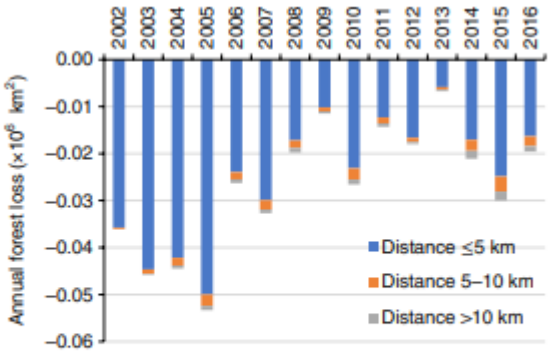

Fig. 4 | Forest loss during 2002–2016 in the Brazilian Amazon. MOD100 evergreen forest-loss area over three distances near areas deforested before 2002 using the geospatial buffer analysis.

The conversion of forests to pasture was associated with 60−80% of Amazon deforestation[17,30,31]. About 62% of the deforested area in MT was converted into pasture during 2001−2004[31]. The cattle count increased substantially from 48×10^6 head in 2000 to 86×10^6 head in 2016 (Supplementary Fig. 4a). Assuming one cow per hectare of pasture[32], the additional number of cattle may occupy 0.38×10^6 km^2 of pasture, which would account for ~94% of the evergreen forest-loss area. MT had the largest increase in cattle (11.4×10^6 head), followed by PA (10.2×10^6 head), RO (8.0×10^6 head) and MA (3.6×10^6 head). Before 2006, the conversion of forests to croplands (for example, soya bean) also contributed to deforestation in the Brazilian Amazon[5,31]. After 2006, croplands were mostly established on previously cleared land[24]. Overall, the four states with the greatest increases in cattle numbers and cropland area also experienced the largest losses of evergreen forests (Supplementary Fig. 4) according to the MOD100 evergreen forest dataset.

Driving factors of evergreen forest area loss

We investigated the factors driving annual forest losses in the MOD100 dataset during 2000–2017 (Supplementary Fig. 5). Annual forest losses corresponded well to climate parameters, and the standardized cross-correlation coefficients (lag = 0) were −0.89, 0.92 and 0.96 between annual deforestation rate and annual precipitation, TWS_{min} and active fire area, respectively (Supplementary Fig. 6). This cross-correlation suggested that annual forest loss was higher in dry years, especially during the strong El Niño years (2010 and 2015/2016) (Fig. 2b, Supplementary Figs. 5a–c and 7). The deforested area in 2010 and 2015/2016 were about 2.3 and 3.7 times higher than the deforested area in 2009 and 2013, respectively. However, the PRODES dataset did not indicate obvious increases of deforested area in 2010 and 2015/2016.

During these drought years, the data from the Tropical Rainfall Measuring Mission (TRMM) and the Gravity Recovery and Climate Experiment (GRACE) showed remarkably low annual precipitation and annual TWS_{min} (Supplementary Fig. 5b), in addition to substantial increases in fire activity and burned area (Fig. 2e). We also found that in the non-drought years (2006, 2008, 2009, 2011 and 2013), about 23% of the deforested areas experienced fires in the same year that deforestation occurred. In the drought years, however, deforested areas often experienced more fire (36%) in the same year (Supplementary Figs. 8a,9 and 10). About 70% of evergreen forests had a fire history before deforestation (Supplementary Fig. 8b). Forests in the Amazon can be degraded over time due to successive fires, drought and selective logging[16,33]. These degraded forest stands can then become more vulnerable to future drought and fire. The relatively dry states (PA, RO, MT and MA) in the ‘Arc of Deforestation’ (Supplementary Fig. 5d), corresponded well to GRACE TWS_{min} and fire activity (Fig. 3). Although the wet states (AM, AP and RR) in northern Brazilian had relatively

small areas of deforestation, they also experienced increased deforestation in severe drought years.

Annual gain of evergreen forest areas

We defined forest gain as non-forested area that was converted into continuous forest for ≥4 years (ref. [25]). During 2001–2013 the MOD100 dataset showed a total gain of 0.071×10^6 km^2 in evergreen forest area in the Brazilian Amazon (Figs. 1f and 2b). This study reported the annual dynamics of both deforestation and reforestation in the Brazilian Amazon using time-series image data and time-series algorithms. Reforestation area, although relatively small, did partially offset deforestation by 21% in the Brazilian Amazon during 2001–2013, which indicates that reforestation played an important role in reducing net forest loss and carbon emissions.

Annual forest area dynamics within protected areas

In an effort to conserve forests in the Brazilian Amazon, protected areas (PAs) have increased from 1.09×10^6 km^2 in 2000 to 2.32×10^6 km^2 in 2013 (Fig. 5), which accounted for 43% of the total land area of the Brazilian Amazon. We analysed annual evergreen forest area dynamics within PAs of the Brazilian Amazon during 2000–2017. PAs sheltered about 50% of the total evergreen forest area in the Brazilian Amazon in 2013. Total evergreen forest area within PAs decreased slightly from 1.98×10^6 km^2 in 2000 to 1.96×10^6 km^2 in 2017 (~1.3% loss over 17 years) (Fig. 5c). This small change in forest area clearly demonstrates the critical role of PAs in forest conservation. When we analysed annual evergreen forest maps, the cumulative deforested area within PAs was 0.044×10^6 km^2, accounting for ~11% of total forest area loss (0.41×10^6 km^2) and the cumulative reforestation within PAs, 0.014×10^6 km^2, ~20% of total forest area gain (0.071×10^6 km^2). In comparison, evergreen forest area in non-PAs decreased substantially from 1.95×10^6 km^2 in 2000 to 1.64×10^6 km^2 in 2017 (Fig. 5c). Deforestation within/around PAs occurred throughout the study period, rendering them fragmented, isolated and under increased threat of further deforestation (Fig. 5b). Previous studies analysed deforestation data during 1998–2010 and reported that PAs reduced deforestation and carbon emissions[34,35]. As various socio-ecological factors influence illegal (and legal) deforestation in PAs, our results could be used to strengthen the governance of PAs in the Brazilian Amazon.

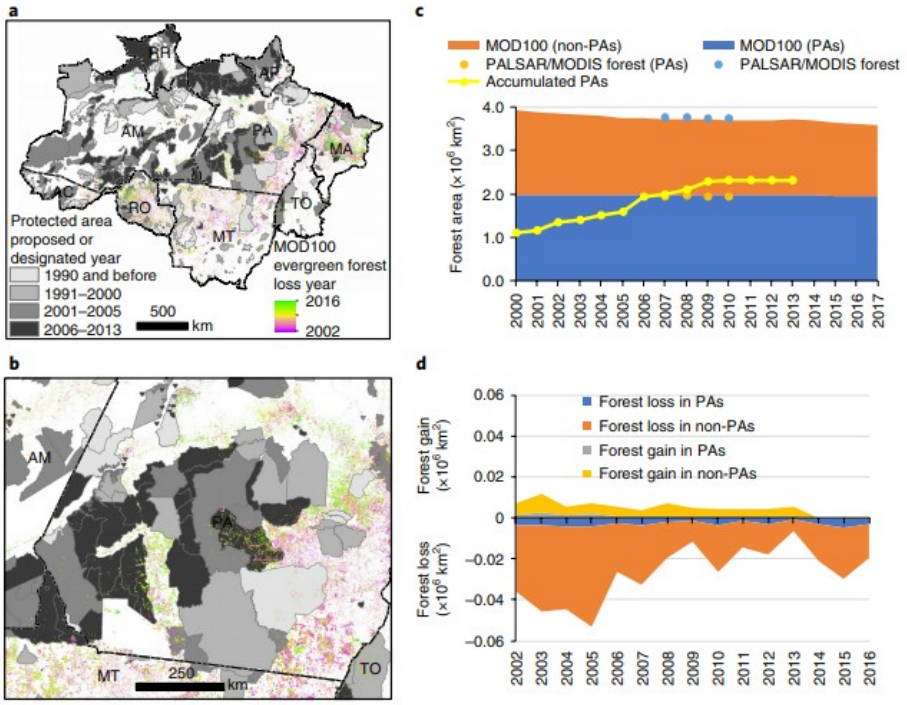

Fig. 5 | Annual dynamics of forest areas within PAs and non-PAs in the Brazilian Amazon during 2000–2017. a, The proposed or designated year for the PAs and the forest-loss year from the MOD100 dataset. **b**, A zoom-in window from **a**. **c**, The forest area changes within the PAs and non-PAs from the MOD100 and PALSAR/MODIS datasets and the accumulated areas of PAs in the Brazilian Amazon during 2000–2013. **d**, Forest loss and gain within the PAs and non-PAs. Credit: PAs maps, UN Environment / IUCN (**a**,**b**)

Discussion

Our results show large discrepancies between PALSAR/MODIS forest product and the Landsat-based forest product (PRODES). We investigated to what degree cloud cover and shadow affected optical images in terms of the number of good-quality observations in 1 year in the Brazilian Amazon (Fig. 6). Analysis of all Landsat images in 2010 shows that a number of pixels in the Brazilian Amazon do not have good-quality observations in 1 year due to cloud cover and shadow (Fig. 6). In addition, about 178–210 Landsat images (path/row) were used in PRODES before 2009 and about 228 Landsat images (path/row) have been used since 2009 (Supplementary Fig. 11). Approximately 5–15% of the area captured by Landsat images still had cloud cover (Supplementary Fig. 11). In comparison, almost all MODIS pixels had good-quality observations in 1 year due to its daily revisit cycles. Those Landsat pixels with no or few good-quality observations in 1 year contributed to the smaller estimates of forest areas reported by PRODES (Supplementary Fig. 2). For those Landsat pixels with no or few good-quality observations in 1 year, GFW used cloud-free observations in neighbouring year(s), which contributed to the uncertainty in annual forest area estimates reported by GFW. We also carried out accuracy assessments of these forest data products using common reference datasets (see Supplementary Information). The PALSAR/MODIS and GFW datasets have similar overall accuracy of ~90% and are higher than that of PRODES (~80%)

(Supplementary Table 3). The PRODES forest had a noticeable omission error (~25%) in forest area estimates in 2010 (Supplementary Table 3). Our PALSAR/MODIS forest maps suggested that the Brazilian Amazon may have substantially more forest area than estimated by the PRODES dataset, which has been widely used in many scientific studies[5,8,34] and in public policy development.

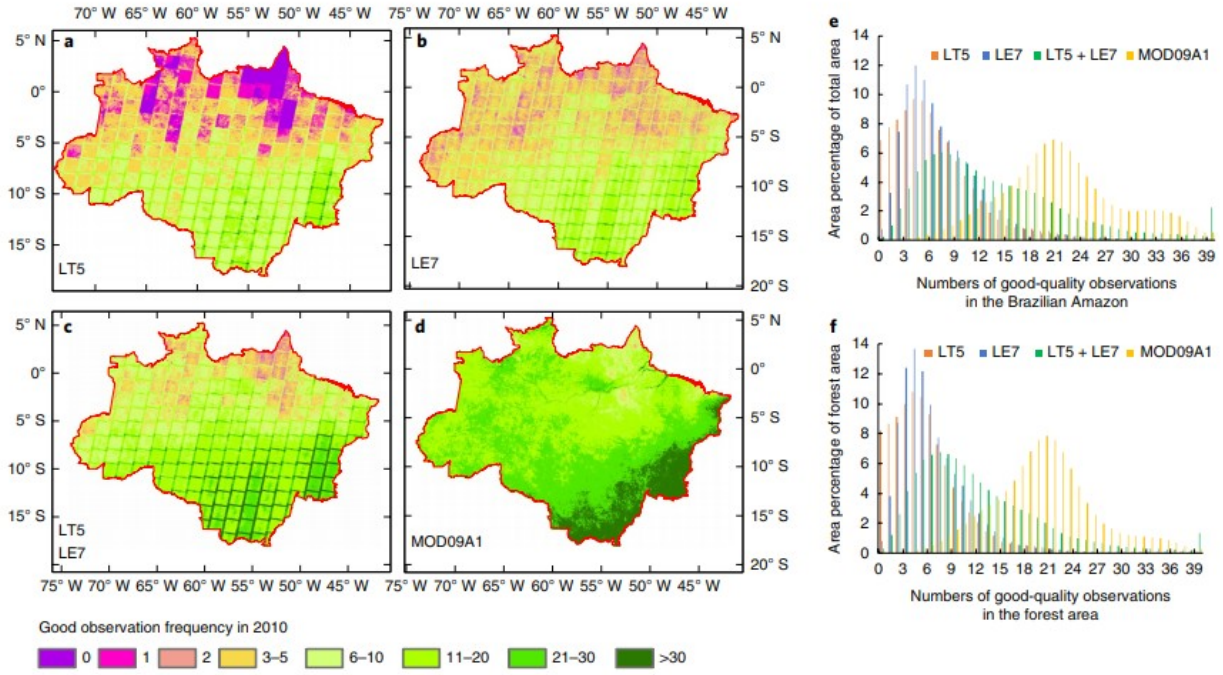

Fig. 6 | Numbers and frequency of good-quality observations in one year from Landsat 5 TM (LT5), Landsat 7 ETM+ (LE7), LT5 + LE7 and MOD09A1 land surface reflectance in the Brazilian Amazon in 2010. a, Numbers of good-quality observations from all LT5 land surface reflectance images. **b**, Numbers of good-quality observations from all LE7 land surface reflectance images. **c**, Numbers of good-quality observations from the combination of all LT5 and LE7 land surface reflectance images. **d**, Numbers of good-quality observations from all MOD09A1 land surface reflectance images[60]. **e**, Frequency of good-quality observations in the Brazilian Amazon. **f**, Frequency of good-quality observations in the PALSAR/MODIS forest area in the Brazilian Amazon. Credit: USGS/NASA Landsat Programme provides LT5 and LE7 land surface reflectance images for **a**–**c**.

Three publications reported the underestimation of forest area loss in the PRODES data and likely casual factors[15,17,36]. The larger estimate of evergreen forest loss from the MOD100 dataset accentuates the likelihood of underestimates in other existing data products, specifically PRODES. The PRODES forest product had high omission errors of about 40% and 28% in 2000 and 2010, respectively (Supplementary Table 3), which can be attributed, to a large degree, to the spatial extent of satellite images to identify forest and the fact that Landsat images have a number of pixels with no good-quality observations in 1 year (Supplementary Fig 11). PRODES forest data has a minimum mapping unit of 6.25 ha, thus it would not account for forest loss in small patches[15,36]. Compared with GFW and MOD100, PRODES underestimated forest-loss area by 67–127%. Landsat 7 Enhanced Thematic Mapper Plus (ETM +) images used in the GFW forest-loss dataset also had a fair number of pixels with no or few good-quality observations in 1 year. For example, about 13.5% of forest area had less

than three good-quality observations in 2010 (Fig. 6). The phenological characteristics of many land cover types could be similar for some time periods in the Brazilian Amazon[37], and thus a limited amount of good-quality observations in 1 year could result in an underestimation of forest-loss area. About 27% of forest-loss area in the PRODES dataset was not identified in the GFW dataset during 2001–2013[15]. In comparison, the MOD100 product used all the observations in 1 year (full or dense time-series) from MOD09A1, which has six or more good-quality observations over 99% of the pixels (Supplementary Fig. 11).

Our results reported forest area gain in the Brazilian Amazon. Various forest restoration projects were carried out in the Brazilian Amazon, most of which focused primarily on commercial plantations, such as eucalyptus, pine and rubber[38]. Compared to native forests, commercial plantations usually have small species richness and simple canopy structure, which have very limited values for biodiversity conservation[39,40,41,42]. The largest tropical reforestation project in recent history was launched in late 2017 by Conservation International, the Brazilian Ministry of Environment, the Global Environment Facility, the World Bank and the Brazilian Biodiversity Fund with the aim to plant 73×10^6 trees in the Brazilian Amazon by 2023. Under the Paris Climate Agreement, Brazil has committed to restoring or reforesting 0.12×10^6 km^2 of land by 2030. Our approaches for mapping the spatio-temporal changes of forests could identify the areas with successful and unsuccessful reforestation efforts and provide valuable information for reforestation projects.

In conclusion, this study demonstrates the potential of time-series microwaves, optical images and algorithms to characterize forest areas in the Brazilian Amazon. The resultant datasets could have important implications for not only land-use policy, management and conservation, but also our understanding of the terrestrial carbon cycle, hydrology and climate. Recent development and policy changes in Brazil, such as the changes to the forest code—the proposed one-sentence constitutional amendment (PEC-65)—and the large-scale construction of dams and highways probably threaten environmental protection policies and efforts that aim to conserve the forest in the Brazilian Amazon[43,44]. If the Brazilian government's deforestation target is to be met (0.004×10^6 km^2 yr^{-1})[30], concrete efforts must be made to improve our capacity for monitoring, reporting and verifying deforestation and reforestation, and to reverse the sharply increasing trend in forest loss over the past few years.

Methods

Remote sensing data

PALSAR data

The PALSAR onboard the ALOS satellite was launched on 14 January 2006. The annual 50-m PALSAR mosaic products are in the Fine Beam Dual (FBD)

polarization mode (HH and HV dual polarizations) and have been slope-corrected, orthorectified and radiometrically calibrated[19,45]. HH means that microwave energy was transmitted and received in the horizontal direction by the antenna and HV means that microwave energy was transmitted in the horizontal direction and received in the vertical direction. We converted the digital number (DN) values into gamma-naught backscattering coefficient in decibels (γ°) using a calibration coefficient (equation (1)).

$$\gamma^{\circ} = 10 \times \log_{10} < \mathrm{DN}^2 > + \mathrm{CF} \qquad (1)$$

where CF is the absolute calibration factor of –83. We further calculated PALSAR difference (equation (2)) and ratio (equation (3)) layers as:

$$\mathrm{Difference} = \mathrm{HH} - \mathrm{HV} \qquad (2)$$

$$\mathrm{Ratio} = \mathrm{HH}/\mathrm{HV} \qquad (3)$$

A number of studies have reported that PALSAR backscattering coefficients are sensitive to tree structure and can be used to generate annual maps of forests[12,19,27,28] and to estimate forest above-ground biomass in different climate regions[46,47,48].

MOD13Q1 Normalized Difference Vegetation Index (NDVI)

The MODIS/Terra MOD13Q1 data are a composite product with the best quality pixel in each 16-d window from daily observations. MOD13Q1 products include the NDVI and Enhanced Vegetation Index (EVI)[49]. The MOD13Q1 NDVI and EVI products are computed from atmospherically corrected bi-directional surface reflectance, which has been masked for water, clouds, heavy aerosols and cloud shadows. NDVI is calculated as a normalized ratio between the red and near-infrared (NIR) surface reflectance. A 16-bit vegetation index quality is provided in the dataset, and only good-quality observations were used in this study.

MOD09A1 data and vegetation indices

The MOD09A1 (v.006) data product has seven land surface spectral bands and contains 1-d observations within an 8-d period. The MOD09A1 has a 16-bit surface reflectance data quality description. We used the MOD09A1 standard data quality flags to identify observations covered by cloud (cloudy and mixed), internal cloud, cloud shadow, high aerosols, high cirrus or snow. We treated those observations with the above-mentioned quality flags as bad observations and excluded them from the time-series data analysis. In addition, we also treated those observations with blue band surface reflectance value >0.20 as bad observations and excluded them from data analysis. Over 99.9% of the MOD09A1 dataset had two or more good-quality

observations in the Brazilian Amazon (Supplementary Fig. 12). We calculated three vegetation indices: NDVI (equation (4)), EVI (equation (5)) and Land Surface Water Index (LSWI) (equation (6))[50] using blue, red, NIR (841–875 nm) and shortwave-infrared (SWIR) (1628–1652 nm) bands.

$$\mathrm{NDVI} = \frac{\rho_{\mathrm{NIR}} - \rho_{\mathrm{red}}}{\rho_{\mathrm{NIR}} + \rho_{\mathrm{red}}} \tag{4}$$

$$\mathrm{EVI} = 2.5 \times \frac{\rho_{\mathrm{NIR}} - \rho_{\mathrm{red}}}{\rho_{\mathrm{NIR}} + 6 \times \rho_{\mathrm{red}} - 7.5 \times \rho_{\mathrm{blue}} + 1} \tag{5}$$

$$\mathrm{LSWI} = \frac{\rho_{\mathrm{NIR}} - \rho_{\mathrm{SWIR}}}{\rho_{\mathrm{NIR}} + \rho_{\mathrm{SWIR}}} \tag{6}$$

where ρ_{blue}, ρ_{red}, ρ_{NIR} and ρ_{SWIR} represent land surface reflectance values from MOD09A1 blue, red, NIR and SWIR bands, respectively.

Precipitation data from TRMM

We calculated annual precipitation during 2001–2016 using observations from TRMM, a joint mission between NASA and JAXA. We used the precipitation from the TRMM 34B2 product with a 3-h temporal resolution and a 0.25-degree spatial resolution[51].

TWS data from GRACE

The 1° GRACE Tellus Monthly Mass Grids provide monthly gravitational anomalies, which have units of ‘Equivalent Water Thickness’, indicating the deviations of mass in terms of the vertical extent of water in centimetres[52,53]. We calculated annual TWS from the 1° GRACE (GRACE $\mathrm{TWS}_{\mathrm{min}}$) Tellus Monthly Mass Grids dataset from 2002 to 2016 in the Brazilian Amazon.

Active fire and burned area data

The active fire and burned area data were from MOD14A2 (Terra Thermal Anomalies & Fire 8-Day Global 1 km, v.006)[54] and MCD64A1 (MODIS Burned Area Monthly Global 500 m, v.006)[55], respectively. We selected active fire with nominal and high confidence levels and burned areas with sufficient valid data in the reflectance time-series in this study. We then generated annual active fire and burned area binary maps if the active fire and burned areas occurred in 1 year in the Brazilian Amazon, respectively.

Multiple forest maps

PALSAR/MODIS forest maps (2007–2010)

We used the FAO’s forest definition in our forest mapping studies: forest as a land parcel (≥0.5 ha) covered by 10% or more tree cover with tree height ≥5 m at their maturity. We developed a new and robust decision tree approach

that combined PALSAR images (50 m) and MOD13Q1 $NDVI_{max}$ images (250 m) to identify and map forests. We used this to generate annual maps of forests at 50-m spatial resolution in China[28], monsoon Asia[27] and South America[12]. The resultant annual PALSAR/MODIS forest maps have been evaluated with extensive ground reference data interpreted from in situ global positioning system-based field photos and Very High Resolution (VHR) images and compared with other forest products and national forest inventory data. In this study, we used annual maps of forests in South America during 2007–2010 from the Forest-PALSAR/MODIS approach[12], and the Brazilian Amazon boundary map was used to subset the South American forest maps.

MOD100 evergreen forest maps (2000–2017)

We used three freely available datasets as the input datasets for algorithm training in 2010: (1) the Global Land Cover Validation Reference Dataset (GLCVRD), (2) MCD12Q1 land cover product and (3) ESA CCI land cover product. The GLCVRD dataset was produced from analyses of VHR images (QuickBird-2, WorldView-1/2, IKONOS-2 and GeoEye-1) acquired mostly in 2010 and based on a stratified random sampling design[56,57,58]. There are 18 sites in the Brazilian Amazon and each of them covers an area of about 5×5 km^2 at a 2-m spatial resolution (Supplementary Fig. 13). The GLCVRD has five land cover types (Tree, Water, Barren, Other Vegetation and Ice & Snow) and two non-land cover types (Cloud and Shadow). We grouped the five land classes into two layers (tree, non-tree) and the two non-land cover types into one class (bad observations) for each site's map and converted their universal transverse mercator projection into an 'equal-area projection' (that is, South_America_Albers_Equal_Area_Conic). We aggregated the tree, non-tree and bad observations layers into the same spatial resolution as MOD09A1 (500 m) and calculated their percentage area fraction within individual pixels. We excluded those pixels with more than 1% area of bad observations, and a total of 966 pixels at MODIS 500-m spatial resolution were selected for algorithm training. For those areas covered by the GLCVRD dataset, we selected evergreen forest and non-evergreen forest training samples within evergreen forest and non-evergreen forest boundaries derived from MCD12Q1 and ESA CCI land cover products.

A unique physical feature of evergreen forests is that they have green leaves all year. Conversely, deciduous forests usually have few or no green leaves during the dry season or winter season, leaving soils and tree trunks to be observed by space-borne sensors. We developed and reported a new, simple and robust algorithm that generated annual maps of tropical evergreen forests in the pantropical zone and monsoon Asia based on the canopy phenology from analyses of time-series water-related LSWI and greenness-related EVI calculated from the MOD09A1 product[26,27]. The Forest-MODIS algorithm is well documented in our previous studies[26,27]. First, we counted the number of good-quality observations that had no cloud (cloudy and mixed), internal cloud, cloud shadow, high aerosols, high cirrus or snow (equation (7)). Second, of those good-quality observations, we counted the

number of observations with LSWI ≥ 0 (equation (8)). Third, we calculated the percentage of observations with LSWI ≥ 0 out of all good observations in 1 year (equation (9)). Fourth, we calculated the minimum EVI values in those good-quality observations in 1 year (equation (10). In this study, we applied this Forest-MODIS algorithm ($PCT_{LSWI \geq 0} = 100\%$ and $EVI_{min} \geq 0.2$; ref. [26]) (Supplementary Fig. 14) to MOD09A1 time-series data in individual years during 2000–2017 and generated annual maps of evergreen forest in the Brazilian Amazon (Fig. 1c) in the web-based cloud computing platform Google Earth Engine. Our Forest-MODIS algorithm is sensitive to evergreen forest loss (Supplementary Fig. 15) and gain (Supplementary Fig. 16).

$$N_{\text{Good-quality observation}} = \sum_{i=1}^{n} (O_i) \tag{7}$$

$$M_{\text{LSWI} \geq 0} = \sum_{j=1}^{m} (O_j) \tag{8}$$

$$\text{PCT}_{\text{LSWI} \geq 0} = \frac{M_{\text{LSWI} \geq 0}}{N_{\text{Good-quality observation}}} \times 100 \tag{9}$$

$$\text{EVI}_{\text{min}} = \min (O_1, O_2, \ldots, O_i, \ldots, O_n) \tag{10}$$

$$0 \leq n \leq 46,\ 0 \leq m \leq 46.$$

where $N_{\text{Good-quality observation}}$, $M_{\text{LSWI} \geq 0}$, $\text{PCT}_{\text{LSWI} \geq 0}$ and EVI_{min} are the number of good-quality observations, the number of observations with LSWI ≥ 0 from good-quality observations, the percentage of observations with LSWI ≥ 0 out of all good observations in one year and the minimum EVI (EVI_{min}) values of those good-quality observations in one year, respectively. O_1, O_2, O_i, O_j, and O_n are the 1st, 2nd, *i*th, *j*th and *n*th individual observation in one year, respectively.

Deforestation is the process of converting forest into non-forest. Reforestation is the process of non-forest being reforested or afforested. Short-rotation industrial plantation (for example, eucalypt) usually has a cycle of 4–6 years[25], thus we defined reforestation as an area converted from non-forest into forest for at least 4 years. We developed an approach to identify and map evergreen forest change (deforestation and reforestation) in the Brazilian Amazon based on the annual MOD100 evergreen forests. This approach includes three steps: (1) we masked out those MOD100 pixels lacking any good-quality observation, (2) we applied a three-observation moving window filter and reduced random errors in the MOD100 evergreen

forest maps and (3) we identified and mapped the location and date for deforestation (equation (11)) and reforestation (equation (12)) based on the refined MOD100 evergreen forest maps during 2001–2016.

$$\text{Deforestation}_{k+1} = \left\{ \begin{array}{c} \text{MOD100}_k = F, \\ \text{MOD100}_{k+1} = \text{NF}, \\ \text{MOD100}_{k+2} = \text{NF} \end{array} \right\} \tag{11}$$

$$\text{Reforestation}_{k+1} = \left\{ \begin{array}{c} \text{MOD100}_k = \text{NF}, \\ \text{MOD100}_{k+1} = F, \\ \text{MOD100}_{k+2} = F \\ \text{MOD100}_{k+3} = F \\ \text{MOD100}_{k+4} = F \end{array} \right\} \tag{12}$$

where MOD100 is the evergreen forest maps, *F* and NF are the abbreviations for evergreen forest and non-evergreen forest, respectively, and $k = 2001,\ldots,$ 2016.

JAXA forest maps (2007–2010, 2015–2016)

The 25-m annual JAXA forest maps[19] were produced using PALSAR FBD polarization mode data from June to September during 2007−2010 and 2015−2016. Data pre-processing includes speckle reduction, ortho-rectification and slope correction and intensity equalization between neighbouring strips. In general, a decision tree algorithm was used to generate the JAXA forest maps. First, a 5×5 pixel median filter was used to reduce noise in images, followed by a multi-resolution segmentation. Then, 15 region-specific HV threshold values were determined to identify forest pixels based on the ground references and cumulative distribution functions. We aggregated the 25-m JAXA forest maps to 500-m resolution for comparison with MODIS-based forest maps.

PRODES forest dataset (2000–2016)

The PRODES project at the Brazilian National Institute for Space Research (INPE) has been mapping annual deforestation since 1988 and providing annual remaining forest area estimates for the Brazilian Amazon since 2000. Visual interpretation of Landsat images was used to generate annual deforestation maps during 1988–1999. The digital image classification approach[18] was used to generate annual deforestation maps from 2003 to 2005. The TerraAmazon platform has been used since 2005, which allows PRODES analysis to be more uniform. In general, three steps are used to generate the PRODES products. First, images are selected to be as cloud-free as possible with an acquisition date closest to the reference date (1

August)[18]. The images are then masked to exclude non-forest and previous deforestation, using the previous year's analysis results. Finally, interpreters delineate deforested polygons (shapefile format) in the intact forest of the previous year. In this study, we used the annual forest cover areas during 2000–2017 (Supplementary Table 1) and annual deforestation area statistics in the Brazilian Amazon during 2001–2016, as reported by the INPE. To estimate the total forest area in the Brazilian Amazon, we generated a cloud-free and a maximum spatial extent of forest (Supplementary Fig. 2) using the annual PRODES forest maps during 2007−2010.

GFW forest dataset (2000–2016)

Tree cover product in 2000 and 2010, annual forest loss from 2000 to 2016 and total forest gain from 2000 to 2012 are generated in GFW through the analysis of time-series Landsat ETM + and Operational Land Imager (OLI) images taken during the growing season[11]. Landsat ETM + images from multiple years around 2000 and 2010 were used to retrieve 30-m GFW tree cover for 2000 and 2010 through a decision tree algorithm based on the training datasets, selected percentile values and the slope of the linear regression of band reflectance value versus image date. We calculated GFW forest maps for 2000 and 2010 (Supplementary Fig. 2) as well as forest loss based on a tree cover ≥10%.

MCD12Q1 land cover dataset (2001–2013)

MCD12Q1 (Land Cover Type Yearly L3 Global 500 m Sinusoidal (SIN) Grid) land cover product has five different land cover classification systems. We used the International Geosphere–Biosphere Programme (IGBP) classification[9]. The IGBP classification map was produced using a supervised classification algorithm. The input datasets include a training dataset and the phenology and temporal variability features of land cover types extracted from 500-m aggregated 32-d average nadir Bidirectional Reflectance Distribution Function (BRDF)-adjusted land surface reflectance (NBAR), EVI, land surface temperature (LST) and annual metrics (minimum, maximum and mean values) for EVI, LST and NBAR bands. Post-processing refinements were applied to create the final land cover product, including sample bias correction and spatial explicit prior probability adjustments. IGBP classification map includes five forest types, including evergreen needleleaf forest, evergreen broadleaf forest, deciduous needleleaf forest, deciduous broadleaf forest and mixed forest, which we merged into a single forest layer (Supplementary Fig. 2).

ESA CCI land cover (2000–2015)

The 300-m ESA CCI land cover maps use the Land Cover Classification System developed by the FAO[29]. First, a unique baseline land cover map is generated using 7-d time-series medium resolution imaging spectrometer imagery during 2003–2012. Independently from this baseline, land cover changes are detected at 1 km based on the AVHRR time-series between

1992 and 1999, SPOT-VEGETATION time-series between 1999 and 2013 and PROBA-V data for years 2013, 2014 and 2015. The last step consists of back-dating and updating the 10-year baseline land cover map to produce the 24 annual land cover maps from 1992 to 2015. We used five forest classes in this study: (1) tree cover, broadleaved, evergreen, closed to open (>15%), (2) tree cover, broadleaved, deciduous, closed to open (>15%), (3) tree cover, needle-leaved, evergreen, closed to open (>15%), (4) tree cover, needle-leaved, deciduous, closed to open (>15%) and (5) tree cover, mixed leaf type (broadleaved and needle-leaved) (Supplementary Fig. 2).

Accuracy assessment and inter-comparison of forest area data products

We carried out substantial accuracy assessment and inter-comparison of forest area data products (see Supplementary Information). The MOD100 forest dataset in 2000 and 2010 had an overall accuracy of ~97% (Supplementary Tables 3 and 4), based on the same reference dataset used in accuracy assessment of PALSAR/MODIS, PRODES and GFW. The MOD100 forest-loss dataset had an overall accuracy of ~98% (Supplementary Table 5). The MOD100 forest gain dataset had an overall accuracy, user's accuracy and producer's accuracy of 99.18% (±0.27), 48.72% (±16.22) and 87.06% (±16.36), respectively (Supplementary Table 5).

Data availability

The PALSAR/MODIS forest and MOD100 forest data that support the findings of this study are available from the corresponding author upon request and will be made available to the public. The other datasets are publicly available online (Supplementary Table 6).

References

1. Ochoa-Quintero, J. M., Gardner, T. A., Rosa, I., Ferraz, S. F. D. & Sutherland, W. J. Tresholds of species loss in Amazonian deforestation frontier landscapes. Conserv. Biol. 29, 440–451 (2015).

2. Davidson, E. A. et al. Te Amazon basin in transition. Nature 481, 321–328 (2012).

3. Jenkins, C. N., Pimm, S. L. & Joppa, L. N. Global patterns of terrestrial vertebrate diversity and conservation. Proc. Natl Acad. Sci. USA 110, E2602–E2610 (2013).

4. Fearnside, P. M. Deforestation in Brazilian Amazonia: history, rates, and consequences. Conserv. Biol. 19, 680–688 (2005).

5. Nepstad, D. et al. Slowing Amazon deforestation through public policy and interventions in beef and soy supply chains. Science 344, 1118–1123 (2014).

6. Hansen, M. C. & DeFries, R. S. Detecting long-term global forest change using continuous felds of tree-cover maps from 8-km advanced very high resolution radiometer (AVHRR) data for the years 1982–99. Ecosystems 7, 695–716 (2004).

7. Souza, C., Firestone, L., Silva, L. M. & Roberts, D. Mapping forest degradation in the Eastern Amazon from SPOT 4 through spectral mixture models. Remote Sens. Environ. 87, 494–506 (2003).

8. Hansen, M. C., Shimabukuro, Y. E., Potapov, P. & Pittman, K. Comparing annual MODIS and PRODES forest cover change data for advancing monitoring of Brazilian forest cover. Remote Sens. Environ. 112, 3784–3793 (2008).

9. Friedl, M. A. et al. MODIS Collection 5 global land cover: algorithm refnements and characterization of new datasets. Remote Sens. Environ. 114, 168–182 (2010).

10. Skole, D. & Tucker, C. Tropical deforestation and habitat fragmentation in the Amazon: satellite data from 1978 to 1988. Science 260, 1905–1910 (1993).

11. Hansen, M. C. et al. High-resolution global maps of 21st-century forest cover change. Science 342, 850–853 (2013).

12. Qin, Y. et al. Annual dynamics of forest areas in South America during 2007–2010 at 50-m spatial resolution. Remote Sens. Environ. 201, 73–87 (2017).

13. Reiche, J. et al. Combining satellite data for better tropical forest monitoring. Nat. Clim. Change 6, 120–122 (2016).

14. Rajão, R., Moutinho, P. & Soares, L. Te rights and wrongs of Brazil’s forest monitoring systems. Conserv. Lett. 10, 495–496 (2017).

15. Richards, P., Arima, E., VanWey, L., Cohn, A. & Bhattarai, N. Are Brazil’s deforesters avoiding detection? Conserv. Lett. 10, 470–476 (2017).

16. Asner, G. P. et al. Selective logging in the Brazilian Amazon. Science 310, 480–482 (2005).

17. Tyukavina, A. et al. Types and rates of forest disturbance in Brazilian Legal Amazon, 2000–2013. Sci. Adv. 3, e1601047 (2017).

18. Achard, F. & Hansen, M. C. Global Forest Monitoring from Earth Observation (Taylor & Francis, 2012).

19. Shimada, M. et al. New global forest/non-forest maps from ALOS PALSAR data (2007–2010). Remote Sens. Environ. 155, 13–31 (2014).

20. Reiche, J. et al. Feature level fusion of multi-temporal ALOS PALSAR and landsat data for mapping and monitoring of tropical deforestation and forest degradation. IEEE J. Sel. Top. Appl. Earth Obs. Remote Sens. 6, 2159–2173 (2013).

21. Qin, Y. et al. Quantifying annual changes in built-up area in complex urban-rural landscapes from analyses of PALSAR and Landsat images. ISPRS J. Photogramm. Remote Sens. 124, 89–105 (2017).

22. McDowell, N. G. et al. Global satellite monitoring of climate-induced vegetation disturbances. Trends Plant Sci. 20, 114–123 (2015).

23. Wu, J. et al. Biological processes dominate seasonality of remotely sensed canopy greenness in an Amazon evergreen forest. New Phytol. 217, 1507–1520 (2018).

24. Macedo, M. N. et al. Decoupling of deforestation and soy production in the southern Amazon during the late 2000s. Proc. Natl Acad. Sci. USA 109, 1341–1346 (2012).

25. le Maire, G., Dupuy, S., Nouvellon, Y., Loos, R. A. & Hakarnada, R. Mapping short-rotation plantations at regional scale using MODIS time series: case of eucalypt plantations in Brazil. Remote Sens. Environ. 152, 136–149 (2014).

26. Xiao, X. M., Biradar, C. M., Czarnecki, C., Alabi, T. & Keller, M. A simple algorithm for large-scale mapping of evergreen forests in tropical America, Africa and Asia. Remote Sens. 1, 355–374 (2009).

27. Qin, Y. et al. Mapping forests in monsoon Asia with ALOS PALSAR 50-m mosaic images and MODIS imagery in 2010. Sci. Rep. 6, 20880 (2016).

28. Qin, Y. W. et al. Forest cover maps of China in 2010 from multiple approaches and data sources: PALSAR, Landsat, MODIS, FRA and NFI. ISPRS J. Photogramm. Remote Sens. 109, 1–16 (2015).

29. Land cover CCI Product User Guide v.2 (European Space Agency, 2016).

30. Nepstad, D. et al. Te end of deforestation in the Brazilian Amazon. Science 326, 1350–1351 (2009).

31. Morton, D. C. et al. Cropland expansion changes deforestation dynamics in the southern Brazilian Amazon. Proc. Natl Acad. Sci. USA 103, 14637–14641 (2006).

32. McManus, C. et al. Dynamics of cattle production in Brazil. PLoS ONE 11, e0147138 (2016).

33. Brando, P. M. et al. Abrupt increases in Amazonian tree mortality due to drought–fre interactions. Proc. Natl Acad. Sci. USA 111, 6347–6352 (2014).

34. Soares, B. et al. Role of Brazilian Amazon protected areas in climate change mitigation. Proc. Natl Acad. Sci. USA 107, 10821–10826 (2010).

35. Nolte, C., Agrawal, A., Silvius, K. M. & Soares, B. S. Governance regime and location infuence avoided deforestation success of protected areas in the Brazilian Amazon. Proc. Natl Acad. Sci. USA 110, 4956–4961 (2013).

36. Bustamante, M. M. C. et al. Are Brazil deforesters avoiding detection? Reply to Richards et al. 2016. Conserv. Lett. 10, 493–494 (2017).

37. Rodrigues, A., Marcal, A. R. S., Furlan, D., Ballester, M. V. & Cunha, M. Land cover map production for Brazilian Amazon using NDVI SPOT VEGETATION time series. Can. J. Remote Sens. 39, 277–289 (2013).

38. Brazil Market Overview: Timber and Forest Products (Hancock Timber Resource Group, 2014).

39. Barlow, J. et al. Diversity and composition of fruit-feeding butterfies in tropical Eucalyptus plantations. Biodivers. Conserv. 17, 1089–1104 (2008).

40. Marsden, S. J., Whifn, M. & Galetti, M. Bird diversity and abundance in forest fragments and Eucalyptus plantations around an Atlantic forest reserve, Brazil. Biodivers. Conserv. 10, 737–751 (2001).

41. Barlow, J. et al. Quantifying the biodiversity value of tropical primary, secondary, and plantation forests. Proc. Natl Acad. Sci. USA 104, 18555–18560 (2007).

42. Coelho, M., Juen, L. & Mendes-Oliveira, A. C. Te role of remnants of Amazon savanna for the conservation of neotropical mammal communities in eucalyptus plantations. Biodivers. Conserv. 23, 3171–3184 (2014).

43. Fearnside, P. M. Brazilian politics threaten environmental policies. Science 353, 746–748 (2016).

44. Freitas, F. L. M. et al. Potential increase of legal deforestation in Brazilian Amazon afer Forest Act revision. Nat. Sustain. 1, 665–670 (2018).

45. Shimada, M., Isoguchi, O., Tadono, T. & Isono, K. PALSAR radiometric and geometric calibration. IEEE Trans. Geosci. Remote Sens. 47, 3915–3932 (2009).

46. Carreiras, J. M. B., Vasconcelos, M. J. & Lucas, R. M. Understanding the relationship between aboveground biomass and ALOS PALSAR data in the forests of Guinea-Bissau (West Africa). Remote Sens. Environ. 121, 426–442 (2012).

47. Cartus, O., Santoro, M. & Kellndorfer, J. Mapping forest aboveground biomass in the Northeastern United States with ALOS PALSAR dualpolarization L-band. Remote Sens. Environ. 124, 466–478 (2012).

48. Ma, J. et al. Estimating aboveground biomass of broadleaf, needleleaf, and mixed forests in Northeastern China through analysis of 25-m ALOS/PALSAR mosaic data. For. Ecol. Manage. 389, 199–210 (2017).

49. Huete, A. R., Liu, H. Q., Batchily, K. & vanLeeuwen, W. A comparison of vegetation indices over a global set of TM images for EOS-MODIS. Remote Sens. Environ. 59, 440–451 (1997).

50. Xiao, X. et al. Observation of fooding and rice transplanting of paddy rice felds at the site to landscape scales in China using VEGETATION sensor data. Int J. Remote Sens. 23, 3009–3022 (2002).

51. Hufman, G. et al. Integrated Multi-satellitE Retrievals for GPM (IMERG) Version 4.4 (NASA’s Precipitation Processing Center, 2014); fp://arthurhou.pps.eosdis.nasa.gov/gpmdata/

52. Swenson, S. C. GRACE monthly land water mass grids NETCDF RELEASE 5.0. CA, USA (NASA Jet Propulsion Laboratory, 2012).

53. Landerer, F. W. & Swenson, S. C. Accuracy of scaled GRACE terrestrial water storage estimates. Water Resour. Res. 48, 4531 (2012).

54. Giglio, L. & Justice, C. MOD14A2 MODIS/Terra Termal Anomalies/Fire 8-Day L3 Global 1km SIN Grid V006 (NASA EOSDIS Land Processes DAAC, 2015); https://doi.org/10.5067/MODIS/MOD14A2.006

55. Giglio, L., Justice, C., Boschetti, L. & Roy, D. MCD64A1 MODIS/Terra+Aqua Burned Area Monthly L3 Global 500m SIN Grid V006 (NASA EOSDIS Land Processes DAAC, 2015); https://doi.org/10.5067/MODIS/MCD64A1.006

56. Pengra, B., Long, J., Dahal, D., Stehman, S. V. & Loveland, T. R. A global reference database from very high resolution commercial satellite data and methodology for application to Landsat derived 30 m continuous feld tree cover data. Remote Sens. Environ. 165, 234–248 (2015).

57. Olofsson, P. et al. A global land-cover validation data set. Part I: fundamental design principles. Int. J. Remote Sens. 33, 5768–5788 (2012).

58. Stehman, S. V., Olofsson, P., Woodcock, C. E., Herold, M. & Friedl, M. A. A global land-cover validation data set. Part II: augmenting a stratifed sampling design to estimate accuracy by region and land-cover class. Int. J. Remote Sens. 33, 6975–6993 (2012).

59. Didan, K. MOD13Q1 MODIS/Terra Vegetation Indices 16-Day L3 Global 250m SIN Grid V006 (NASA EOSDIS Land Processes DAAC, 2015); https://doi.org/10.5067/MODIS/MOD13Q1.006

60. Vermote, E. MOD09A1 MODIS/Terra Surface Refectance 8-Day L3 Global 500m SIN Grid V006 (NASA EOSDIS Land Processes DAAC, 2015); https://doi.org/10.5067/MODIS/MOD09A1.006

Acknowledgements

This study is supported in part by research grants from NASA Land Use and Land Cover Change programme (grant no. NNX14AD78G), NASA Geostationary Carbon Cycle Observatory (GeoCarb) Mission (GeoCarb Contract no. 80LARC17C0001), the Inter-American Institute for Global Change Research (IAI) (grant no. CRN3076), which is supported by the US National Science Foundation (grant no. GEO-1128040) and NSF EPSCoR project (no. IIA-1301789).